



# Syntheses, structures and bioactivities of silver(I) complexes with dithioether ligands that contain a di- or triethylene glycol chain and different terminal groups

Yan An<sup>a</sup>, Xiaofeng Li<sup>a,\*</sup>, Huiguo Chen<sup>a,b</sup>, Weisheng Liu<sup>b</sup>, Seikweng Ng<sup>c</sup>, Yuliang Zhang<sup>a</sup>, Junhua Wang<sup>a</sup>

<sup>a</sup> Institute of Marine Materials Science and Engineering, Shanghai Maritime University, Shanghai 201306, China

<sup>b</sup> Department of Chemistry, State Key Laboratory of Applied Organic Chemistry, College of Chemistry and Chemical Engineering, Lanzhou University, Lanzhou 730000, China

<sup>c</sup> Department of Chemistry, University of Malaya, Kuala Lumpur 50603, Malaysia

## ARTICLE INFO

### Article history:

Received 8 February 2011

Received in revised form 7 June 2011

Accepted 10 June 2011

Available online 13 July 2011

### Keywords:

Dithioethyl ligand

Silver complex

Coordination structure

Inhibitory activity

*Phaeodactylum tricornutum*

## ABSTRACT

A series of flexible dithioethyl ligands that contain ethyleneoxy segments were designed and synthesized, including bis(2-(pyridin-2-ylthio)ethyl)ether (**L**<sup>1</sup>), 1,2-bis(2-(pyridin-2-ylthio)ethoxy)ethane (**L**<sup>2</sup>), bis(2-(benzothiazol-2-ylthio)ethyl)ether (**L**<sup>3</sup>) and 1,2-bis(2-(benzothiazol-2-ylthio)ethoxy)ethane (**L**<sup>4</sup>). Reactions of these ligands with AgNO<sub>3</sub> led to the formation of four new supramolecular coordination complexes, [Ag<sub>2</sub>**L**<sup>1</sup>(NO<sub>3</sub>)<sub>2</sub>]<sub>2</sub> (**1**), [Ag<sub>2</sub>**L**<sup>2</sup>(NO<sub>3</sub>)<sub>2</sub>] (**2**), [Ag**L**<sup>3</sup>(NO<sub>3</sub>)]<sub>∞</sub> (**3**) and [Ag**L**<sup>4</sup>(NO<sub>3</sub>)] (**4**) in which the length of the (CH<sub>2</sub>CH<sub>2</sub>O)<sub>n</sub> spacers and the terminal groups of ligands cause subtle geometrical differences. Studies of the inhibitory effect to the growth of *Phaeodactylum tricornutum* show that all four complexes are active and the compound **4** has the highest inhibitory activity.

© 2011 Elsevier B.V. All rights reserved.

## 1. Introduction

Silver(I) is a favorable building block for various coordination structures which makes the study of silver(I) chemistry very attractive [1–4]. For a long time, the molecular design and structural characterization of silver(I) complexes is an intriguing aspect of bioinorganic chemistry and metal-based drug research [5–9].

Thioether ligands have always been used to form polynuclear complexes with silver(I) for their rich structural information and flexible nature of spacers [10–15]. As demonstrated previously, selecting proper ligands as building blocks is a determining factor in controlling the coordination structures [16–20]. In order to further investigate the coordination construction of silver(I) complexes effected by the introduction of the oxygen atoms into the dithioethyl chain, and the inversion of the terminal groups, as presented herein, we designed and synthesized four flexible dithioethyl ligands that contain ethyleneoxy segments, bis(2-(pyridin-2-ylthio)ethyl)ether (**L**<sup>1</sup>), 1,2-bis(2-(pyridin-2-ylthio)ethoxy)ethane (**L**<sup>2</sup>), bis(2-(benzothiazol-2-ylthio)ethyl)ether (**L**<sup>3</sup>) and 1,2-bis(2-(benzothiazol-2-ylthio)ethoxy)ethane (**L**<sup>4</sup>) (see Scheme 1). The construction of these four novel silver(I) coordination architectures by using these four ligands will be reported hereafter.

As a type of disinfectant, silver–organic complexes have been widely used, but the reports on algae inhibition are rare [21,22].

As shown this article, primary inhibitory effect of the silver complexes we synthesized to the marine diatom *Phaeodactylum tricornutum* is expected to introduce a new method to control the marine red-tide or the marine fouling.

## 2. Experimental

### 2.1. Chemicals and general methods

All the reagents and solvents for synthesis were commercially available and employed without further purification or with purification by standard methods prior to use. ESI-MS spectra were performed on an Esquire 6000 spectrometer, and IR spectra on a 170SX (Nicolet) FTIR spectrometer with KBr pellets. NMR spectra were recorded on a Mercury Plus 400 spectrometer in CDCl<sub>3</sub> solution with TMS as internal standard.

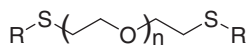
### 2.2. Synthesis of ligands

#### 2.2.1. Bis(2-(pyridin-2-ylthio)ethyl)ether (**L**<sup>1</sup>)

A solution of bis(2-chloroethyl)ether in ethanol was added dropwise to a hot mixture solution of pyridine-2-thiol, KOH in ethanol, and the mixture was further stirred at 80 °C for 5 h. After cooling down, inorganic salts were separated by filtration, and the solvent removed from the filtrate under reduced pressure. The crude product was purified by chromatography on silica using petroleum/ethyl acetate (5:1) as eluent, and the ligand **L**<sup>1</sup> was ob-

\* Corresponding author. Tel.: +86 21 38284804; fax: +86 21 38284800.

E-mail address: xfli@shmtu.edu.cn (X. Li).



$L^1$ :  $n = 1$ , R = pyridyl;  $L^2$ :  $n = 2$ , R = pyridyl;

$L^3$ :  $n = 1$ , R = benzothiazyl;  $L^4$ :  $n = 2$ , R = benzothiazyl

**Scheme 1.** Structures of the ligands used in the study.

tained as a colorless liquid. Yield: 76.6%.  $^1\text{H}$  NMR ( $\text{CDCl}_3$ , 400 MHz):  $\delta$  3.357–3.394 (m, 4H), 3.717–3.750 (m, 4H), 6.904–6.944 (m, 2H), 7.131–7.159 (m, 2H), 7.390–7.437 (m, 2H), 8.361–8.371 (m, 2H).  $^{13}\text{C}$  NMR ( $\text{CDCl}_3$ , 400 MHz):  $\delta$  29.13, 69.71, 119.24, 122.14, 135.71, 149.26, 158.29. ESI-MS:  $m/z$  293.2 [ $L^1\text{H}^+$ ]. IR (KBr,  $\nu$ ,  $\text{cm}^{-1}$ ): 3045m, 2929m, 2857m, 1578vs, 1553s, 1454s, 1414vs, 1356m, 1285m, 1122vs, 1042w, 986w, 758s, 722m.

#### 2.2.2. 1,2-Bis(2-(pyridin-2-ylthio)ethoxy)ethane ( $L^2$ )

$L^2$  was obtained from the reaction of 1,2-bis(2-chloroethoxy)ethane and pyridine-2-thiol with the similar procedure as described above. Yield: 59.5%.  $^1\text{H}$  NMR ( $\text{CDCl}_3$ , 400 MHz):  $\delta$  3.380–3.414 (t, 4H), 3.658–3.660 (d, 4H), 3.731–3.764 (t, 4H), 6.931–6.962 (m, 2H), 7.156–7.178 (m, 2H), 7.422–7.464 (m, 2H), 8.390–8.402 (m, 2H).  $^{13}\text{C}$  NMR ( $\text{CDCl}_3$ , 400 MHz):  $\delta$  29.08, 70.12, 70.14, 119.24, 122.13, 135.72, 149.28, 158.35. ESI-MS:  $m/z$  337.1 [ $L^2\text{H}^+$ ]. IR (KBr,  $\nu$ ,  $\text{cm}^{-1}$ ): 3045w, 2927m, 2864s, 1578vs, 1558s, 1454vs, 1415vs, 1353w, 1285m, 1122vs, 1043w, 986w, 760s, 722m.

#### 2.2.3. Bis(2-(benzothiazol-2-ylthio)ethyl)ether ( $L^3$ )

A solution of bis(2-chloroethyl)ether in ethanol was added dropwise to a hot mixture solution of 2-mercaptobenzothiazole, KOH in ethanol (100 mL), and the mixture was further stirred at 80 °C for 15 h. After cooling down, the precipitate was filtered, washed with ethanol and water, and recrystallized from ethanol to obtain white powder. Yield: 56%.  $^1\text{H}$  NMR ( $\text{CDCl}_3$ , 400 MHz):  $\delta$  3.56 (t, 4H), 3.89 (t, 4H), 7.25 (m, 2H), 7.39 (m, 2H), 7.70 (d, 2H), 7.82 (t, 2H).  $^{13}\text{C}$  NMR ( $\text{CDCl}_3$ , 400 MHz):  $\delta$  32.79, 69.30, 120.88, 121.38, 124.16, 125.92, 135.19, 153.02, 166.34. ESI-MS:  $m/z$  405.0 [ $L^3\text{H}^+$ ]. IR (KBr,  $\nu$ ,  $\text{cm}^{-1}$ ): 3049w, 2903m, 2861m, 1483w, 1458s, 1427vs, 1310w, 1239m, 1102vs, 1034m, 997vs, 752vs, 723m.

#### 2.2.4. 1,2-Bis(2-(benzothiazol-2-ylthio)ethoxy)ethane ( $L^4$ )

$L^4$  was obtained from the reaction of 1,2-bis(2-chloroethoxy)ethane and 2-mercaptobenzothiazole with the similar procedure as described for  $L^3$ . Yield: 46.3%.  $^1\text{H}$  NMR ( $\text{CDCl}_3$ , 400 MHz):  $\delta$  3.538–3.570 (t, 4H), 3.668 (s, 4H), 3.841–3.873 (t, 4H), 7.237–7.275 (t, 2H), 7.360–7.399 (t, 2H), 7.700–7.720 (d, 2H), 7.829–7.849 (d, 2H).  $^{13}\text{C}$  NMR ( $\text{CDCl}_3$ , 400 MHz):  $\delta$  32.84, 69.56, 70.37, 120.87, 121.38, 124.11, 125.90, 135.21, 153.08, 166.43. ESI-MS:  $m/z$  449.1 [ $L^4\text{H}^+$ ]. IR (KBr,  $\nu$ ,  $\text{cm}^{-1}$ ): 3059w, 2929w, 2887m, 2865m, 2812w, 1487w, 1457s, 1425vs, 1321m, 1281m, 1236m, 1125vs, 994vs, 753s, 728m.

### 2.3. Preparation of complexes

#### 2.3.1. $[\text{Ag}_2L^1(\text{NO}_3)_2]_2$ (**1**)

A solution of  $\text{AgNO}_3$  (34.0 mg, 0.2 mmol) in MeOH (5 mL) was added to a solution of  $L^1$  (29.2 mg, 0.1 mmol) in  $\text{CHCl}_3$  (5 mL) in a 25 mL flask and white powder formed immediately. Yield: 56.2%. Single crystals suitable for X-ray analysis were obtained by recrystallization the powder from MeOH/ $\text{CHCl}_3$ /DMF.

#### 2.3.2. $[\text{Ag}_2L^2(\text{NO}_3)_2]$ (**2**)

A solution of  $\text{AgNO}_3$  (34.0 mg, 0.2 mmol) in MeOH (5 mL) was added to a solution of  $L^2$  (33.6 mg, 0.1 mmol) in  $\text{CHCl}_3$  (5 mL) in

a 25 mL flask. The reaction mixture was stirred at room temperature for 4 h and filtered to give a colorless solution in the beaker. The resulted solution was kept in the dark and colorless crystals suitable for X-ray analysis formed at the bottom of the beaker after 5 days. Yield: 50.5%.

#### 2.3.3. $[\text{Ag}L^3(\text{NO}_3)]_\infty$ (**3**)

A solution of  $\text{AgNO}_3$  (17.0 mg, 0.1 mmol) in MeOH (5 mL) was added to a solution of  $L^3$  (40.4 mg, 0.1 mmol) in  $\text{CHCl}_3$  (5 mL) in a 25 mL flask and white powder formed immediately. Yield: 63.5%. Single crystals suitable for X-ray analysis were obtained by recrystallization the powder from MeOH/ $\text{CHCl}_3$ /DMF.

#### 2.3.4. $[\text{Ag}L^4(\text{NO}_3)]$ (**4**)

A solution of  $\text{AgNO}_3$  (17.0 mg, 0.1 mmol) in MeOH (5 mL) was added to a solution of  $L^4$  (44.8 mg, 0.1 mmol) in  $\text{CHCl}_3$  (5 mL) in a 25 mL flask. The reaction mixture was stirred at room temperature for 4 h and filtered to give a colorless solution in the beaker. The resulted solution was kept in the dark and colorless crystals suitable for X-ray analysis formed at the bottom of the beaker after 10 days. Yield: 58.5%.

### 2.4. X-ray crystallography

Single-crystal X-ray diffraction measurements of complex **1** was carried out on a Bruker Smart 1000 CCD diffractometer operating at 50 kV and 30 mA using Mo  $K\alpha$  radiation ( $\lambda = 0.71073 \text{ \AA}$ ), and data collection using the SMART and SAINT software. An empirical absorption correction was applied using the SADABS program. While the data of complexes **2**, **3** and **4** were collected at 293 K using an Oxford Xcalibur S diffractometer with Cu  $K\alpha$  radiation ( $\lambda = 1.54184 \text{ \AA}$ ). Data collection, integration and scaling of the reflections were performed by means of the CRYALIS suite of programs. All the structures of complexes **1–4** were solved by direct methods with SHELXS97 [23] and refined by the full-matrix least-squares method on all  $F^2$  data using the SHELXL-97 [24] programs. All non-hydrogen atoms were refined with anisotropic displacement parameters. The hydrogen atoms were added theoretically and riding on the concerned atoms. Crystallographic data and experimental details for structure analyses are summarized in Table 1.

### 2.5. Antimicrobial activities of the complexes

The bioactivities of the four complexes were assessed by their ability to inhibit the growth of *P. tricornutum* in a medium (pH 8.3) containing filtered artificial sea water (30 g/L of commercial salts),  $\text{Na}_2\text{HPO}_4$  (4.4 mg/L),  $\text{NaNO}_3$  (74.8 mg/L),  $\text{Na}_2\text{SiO}_3$  (16.7 mg/L),  $\text{CuSO}_4 \cdot 5\text{H}_2\text{O}$  (10 mg/L),  $\text{CoCl}_2 \cdot 6\text{H}_2\text{O}$  (12 mg/L),  $\text{MnCl}_2 \cdot 4\text{H}_2\text{O}$  (178 mg/L),  $\text{V}_2\text{MoO}_4 \cdot 2\text{H}_2\text{O}$  (7.3 mg/L),  $\text{Na}_2\text{-EDTA}$  (4.35 g/L), vitamin B1 (100 mg/L), vitamin B12 (0.5 mg/L) and vitamin H (0.5 mg/L). The water was of Milli-Q quality (Millipore).

Erlenmeyer flasks (250-mL) were inoculated with 100 ml ( $2.50 \times 10^6$  cell/mL) of a mother diatom culture. The microalgae were grown under a light–dark cycle (12 h/12 h, illumination: fluorescent tubes, 4000–6000 lux) in a phytotron thermostated at  $18 \pm 1 \text{ }^\circ\text{C}$ .

Different concentrations of the complex (0, 50, 100, 150, 200, 250  $\mu\text{g/L}$ ) were applied the 4th day after inoculation (exponential phase). Measurements were performed 96 h after the complex addition.

**Table 1**  
Crystallographic data and structure refinement summary for complexes **1–4**.

	<b>1</b>	<b>2</b>	<b>3</b>	<b>4</b>
Complexes	[Ag <sub>2</sub> L <sup>1</sup> (NO <sub>3</sub> ) <sub>2</sub> ] <sub>2</sub>	[Ag <sub>2</sub> L <sup>2</sup> (NO <sub>3</sub> ) <sub>2</sub> ]	[AgL <sup>3</sup> (NO <sub>3</sub> )] <sub>∞</sub>	[AgL <sup>4</sup> (NO <sub>3</sub> )]
Chemical formula	C <sub>28</sub> H <sub>32</sub> N <sub>8</sub> O <sub>14</sub> S <sub>4</sub> Ag <sub>4</sub>	C <sub>16</sub> H <sub>20</sub> N <sub>4</sub> O <sub>8</sub> S <sub>2</sub> Ag <sub>2</sub>	C <sub>18</sub> H <sub>16</sub> N <sub>3</sub> O <sub>4</sub> S <sub>4</sub> Ag	C <sub>20</sub> H <sub>20</sub> N <sub>3</sub> O <sub>5</sub> S <sub>4</sub> Ag
Formula weight	1264.38	676.22	574.45	618.50
Crystal system	monoclinic	monoclinic	orthorhombic	orthorhombic
Space group	<i>P</i> 2 <sub>1</sub> / <i>n</i>	<i>C</i> 2/ <i>c</i>	<i>P</i> 2 <sub>1</sub> 2 <sub>1</sub> 2 <sub>1</sub>	<i>P</i> 2 <sub>1</sub> 2 <sub>1</sub> 2 <sub>1</sub>
<i>a</i> (Å)	8.793(4)	31.5690(6)	8.7232(2)	11.9129(2)
<i>b</i> (Å)	13.909(2)	9.5266(1)	11.1390(3)	12.3197(3)
<i>c</i> (Å)	15.974(3)	15.4276(3)	22.4324(5)	16.3594(4)
$\alpha$ (°)	90	90	90	90
$\beta$ (°)	98.96(3)	107.7365(19)	90	90
$\gamma$ (°)	90	90	90	90
<i>V</i> (Å <sup>3</sup> )	1929.8(9)	4419.25(13)	2179.71(10)	2400.97(10)
<i>Z</i>	2	8	4	4
$\mu$ (mm <sup>-1</sup> )	2.293	16.458	11.276	10.318
<i>D</i> <sub>calc</sub> (g/cm <sup>3</sup> )	2.176	2.033	1.750	1.711
<i>T</i> (K)	293(2)	293(2)	293(2)	293(2)
Reflections collected	3787	4312	3109	3895
Unique reflections	3154	3743	2369	3721
<i>R</i> <sub>int</sub>	0.0258	0.0357	0.0320	0.0333
<i>S</i> on <i>F</i> <sup>2</sup>	1.138	1.047	0.995	1.027
<i>R</i> <sub>1</sub> [ <i>I</i> > 2σ( <i>I</i> )] <sup>a</sup>	0.0323	0.0572	0.0350	0.0715
<i>wR</i> <sub>2</sub> [ <i>I</i> > 2σ( <i>I</i> )] <sup>b</sup>	0.0832	0.1604	0.0579	0.1756

$$^a R_1 = \sum ||F_o| - |F_c||/|F_o|.$$

$$^b wR_2 = [\sum w(F_o^2 - F_c^2)^2 / \sum w(F_o^2)^2]^{1/2}.$$

### 3. Results and discussion

#### 3.1. Crystal structures description

##### 3.1.1. [Ag<sub>2</sub>L<sup>1</sup>(NO<sub>3</sub>)<sub>2</sub>]<sub>2</sub> (**1**)

The reaction of AgNO<sub>3</sub> with L<sup>1</sup> led to the formation of a neutral dimeric complex **1**, in which two basic dinuclear units [Ag<sub>2</sub>L<sup>1</sup>(NO<sub>3</sub>)<sub>2</sub>] linked by two NO<sub>3</sub><sup>-</sup> anions into a tetranuclear structure unit (Fig. 1a). A structural feature of the [Ag<sub>2</sub>L<sup>1</sup>(NO<sub>3</sub>)<sub>2</sub>] unit is that the Ag<sup>+</sup> ions have two different coordination geometries. Ag1 is coordinated by two pyridyl N atoms from the ligand, and an O atom from a NO<sub>3</sub><sup>-</sup> anion, forming a T-shaped configuration. Ag2 is coordinated to two S atoms from the ligand, and three O atoms from two NO<sub>3</sub><sup>-</sup> anions to form a five-coordination geometry. It is noteworthy that the short distance (2.9493(6) Å) between the silver cations indicating the existence of Ag–Ag interaction in the dinuclear structure [25]. In the centrosymmetric dimer, two O atoms of one NO<sub>3</sub><sup>-</sup> bridge two dinuclear units through coordinating to the neighboring Ag<sup>I</sup> ions.

Two coordinating O atoms in the NO<sub>3</sub><sup>-</sup> anion and H atoms from adjacent dimers form O(2)···H(4A)–C(4) (Py) intermolecular hydrogen bonds (ca. 2.544 Å). The adjacent pyridine rings from different dimers are parallel to each other with the centroid–centroid distance of ca. 3.673 Å, indicating the presence of face-to-face π–π stacking interactions. The co-effects of O(2)···H(4A)–C(4) (Py) hydrogen bonds and π–π interactions link the dimers into one-dimensional (1-D) chain structure along the *a* direction (Fig. 1b). Furthermore, the other C–H···O hydrogen bonds between adjacent chains extend the 1-D chains into a 3-D framework as depicted in Fig. 1c [26].

##### 3.1.2. [Ag<sub>2</sub>L<sup>2</sup>(NO<sub>3</sub>)<sub>2</sub>]<sub>2</sub> (**2**)

The reaction of AgNO<sub>3</sub> with L<sup>2</sup> led to the formation of a dinuclear complex [Ag<sub>2</sub>L<sup>2</sup>(NO<sub>3</sub>)<sub>2</sub>] **2**, which is basically the same as the basic dinuclear unit of complex **1**, as shown in Fig. 2a. In the dinuclear unit, the Ag<sup>I</sup> ions also have two different coordination geometries, and the L<sup>2</sup> ligand coordinates to two Ag<sup>I</sup> ions to form a dinuclear unit. In **2**, Ag2 is coordinated by two pyridyl N atoms and an O atom from one NO<sub>3</sub><sup>-</sup> anion, showing a trigonal planar geometry. Ag1 has a distorted tetrahedral coordination geometry comprised

of two S atoms and an O atom from the ligand as well as an O atom from another NO<sub>3</sub><sup>-</sup> anion. It is worth being pointed out that the short Ag–Ag distance of 2.9565(6) Å in the dinuclear unit indicates the presence of ligand-supported Ag–Ag interaction which is similar to complex **1** and often observed in Ag<sup>I</sup> complexes.

In complex **2**, uncoordinated O atoms from NO<sub>3</sub><sup>-</sup> anions form C–H···O hydrogen bonds (ca. 2.856 Å) with pyridyl C–Hs which link the dinuclear units into one-dimensional chain structure along the *b* direction (Fig. 2b). The hydrogen bonds (ca. 2.576 Å) between O atoms from NO<sub>3</sub><sup>-</sup> anions and the alkane C–Hs from adjacent dinuclear units, together with the hydrogen bonds (ca. 2.408 Å) between O atoms from NO<sub>3</sub><sup>-</sup> anions and pyridyl C–Hs, stabilize the 3D structure (Fig. 2c) [27].

##### 3.1.3. [AgL<sup>3</sup>(NO<sub>3</sub>)]<sub>∞</sub> (**3**)

The crystal structure of complex **3** features an infinite 1-D chain formed by Ag<sup>I</sup> ions bridged with L<sup>3</sup> along the *a* direction (Fig. 3a). Each Ag<sup>I</sup> ion is coordinated by two N atoms of two benzothiazolyl groups from two distinct L<sup>3</sup> ligands, and two O atoms of NO<sub>3</sub><sup>-</sup>, showing a distorted tetrahedron geometry. The average Ag–N and Ag–O bond distances are 2.2049 and 2.4464 Å, respectively, being in the normal range of analogous complexes with N-containing ligands [28].

In the 1D chain structure of **3**, the adjacent basic repeating unit [AgL<sup>3</sup>(NO<sub>3</sub>)] are linked by the bridges of L<sup>3</sup> ligands with the Ag···Ag distance of 8.831 Å, and L<sup>3</sup> adopts an *N,N*-bidentate bridging mode in *trans*-form (Fig. 3b) [29]. An interesting point is the stacking pattern of **3** in the solid state, the uncoordinated O atom of NO<sub>3</sub><sup>-</sup> forms the acceptor of a C–H···O intermolecular hydrogen bond between the O atom and an aromatic C–H of adjacent chain, which link the complex to form a 3-D supramolecular framework structure (Fig. 3c). The H···O distances are ca. 2.764, 2.605 and 2.953 Å, falling into the range of C–H···O hydrogen bond interactions [30].

##### 3.1.4. [AgL<sup>4</sup>(NO<sub>3</sub>)] (**4**)

The mononuclear complex [AgL<sup>4</sup>(NO<sub>3</sub>)] **4** is composed of a Ag<sup>I</sup> ion, a L<sup>4</sup> ligand and a NO<sub>3</sub><sup>-</sup> anion, as shown in Fig. 4a. In the molecular structure of **4**, the Ag<sup>I</sup> center is coordinated to two N atoms from L<sup>4</sup> and an O atom of NO<sub>3</sub><sup>-</sup>, showing a distorted T-shaped con-

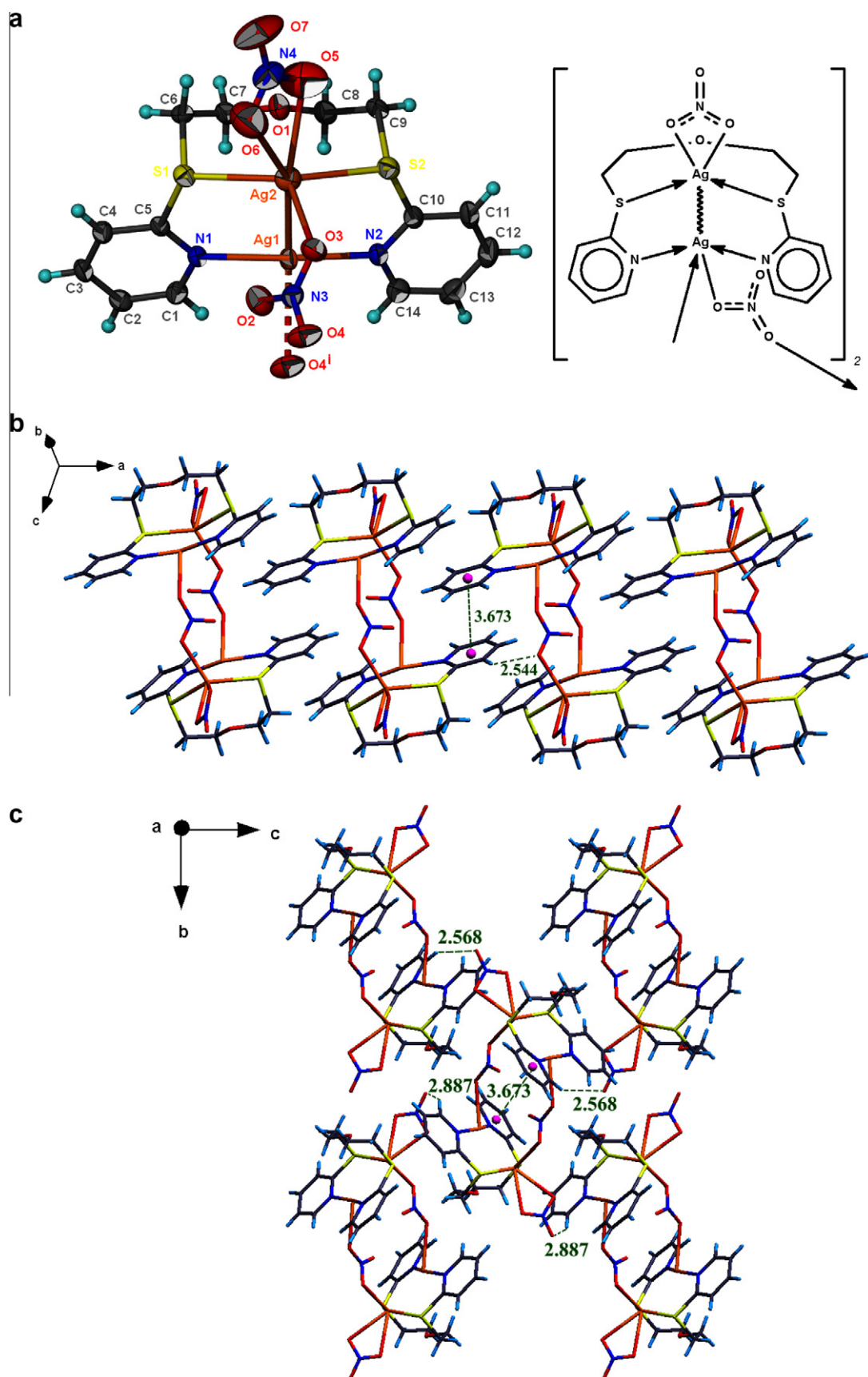


**Fig. 1.** (a) Coordination environment of  $\text{Ag}^{\text{I}}$  ion in **1**. (b) 1D chain in **1**. (c) 3D supramolecular network in **1** linked via C–H...O hydrogen bonds and  $\pi$ – $\pi$  interactions.

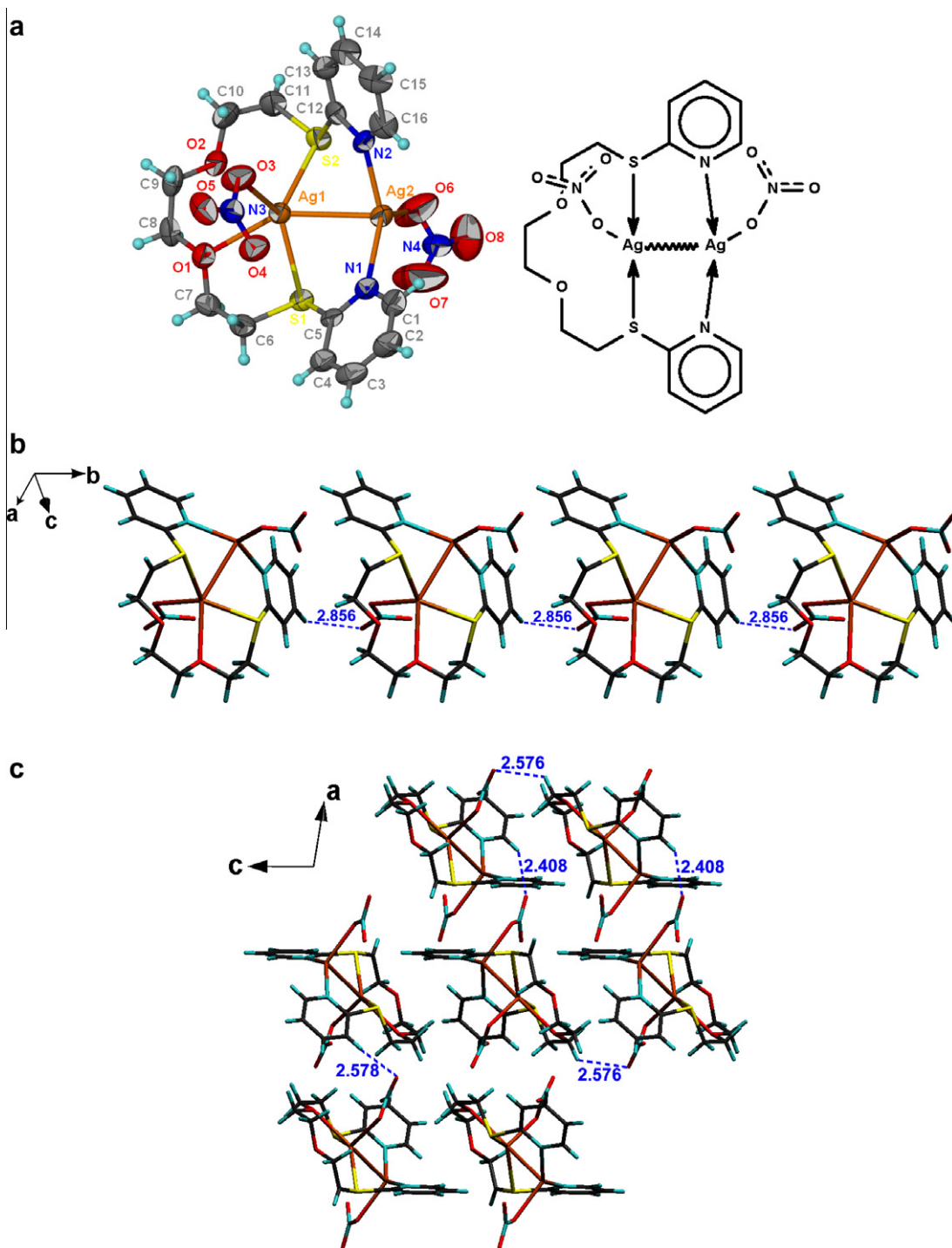


Fig. 2. (a) Coordination environment of  $\text{Ag}^{\text{I}}$  ions in **2**. (b) 1D chain in **2**. (c) 3D supramolecular network in **2** linked via C–H...O hydrogen bonds.

figuration. The ligand **L**<sup>4</sup> adopts an *N,N*-bidentate chelating mode in *cis*-form to coordinate to the  $\text{Ag}^{\text{I}}$  center, while **L**<sup>3</sup> adopts an *N,N*-bidentate bridging mode in *trans*-form in complex **3**. **L**<sup>4</sup> and  $\text{Ag}^{\text{I}}$  ion form a slightly twisted 15-membered macrometallacycle with the Ag atom deviating from the plane by ca. 0.405 Å.

In complex **4**, an uncoordinated O atom of  $\text{NO}_3^-$  and two H atoms on different benzothiazolyl groups in one ligand **L**<sup>4</sup> form two types of C–H...O intramolecular hydrogen bonds (ca. 2.521 and 2.741 Å), which further stabilize the complex into a

one-dimension structure in company with the  $\pi$ – $\pi$  stacking interactions (ca. 3.763 Å) (Fig. 4b).

In addition, the coordinating and uncoordinating O atoms of  $\text{NO}_3^-$  also forms C–H...O (ca. 2.517 and 2.369 Å) intermolecular hydrogen bonds with an alkane C–H from another neighboring mononuclear unit. It is noteworthy that there are weak Ag...S interactions ( $d_{\text{Ag}(1)\cdots\text{S}(1)} = 3.445$  Å) between two adjacent mononuclear units. These intermolecular hydrogen bonds and weak Ag...S interactions extend the mononuclear units into a 3D structure, which

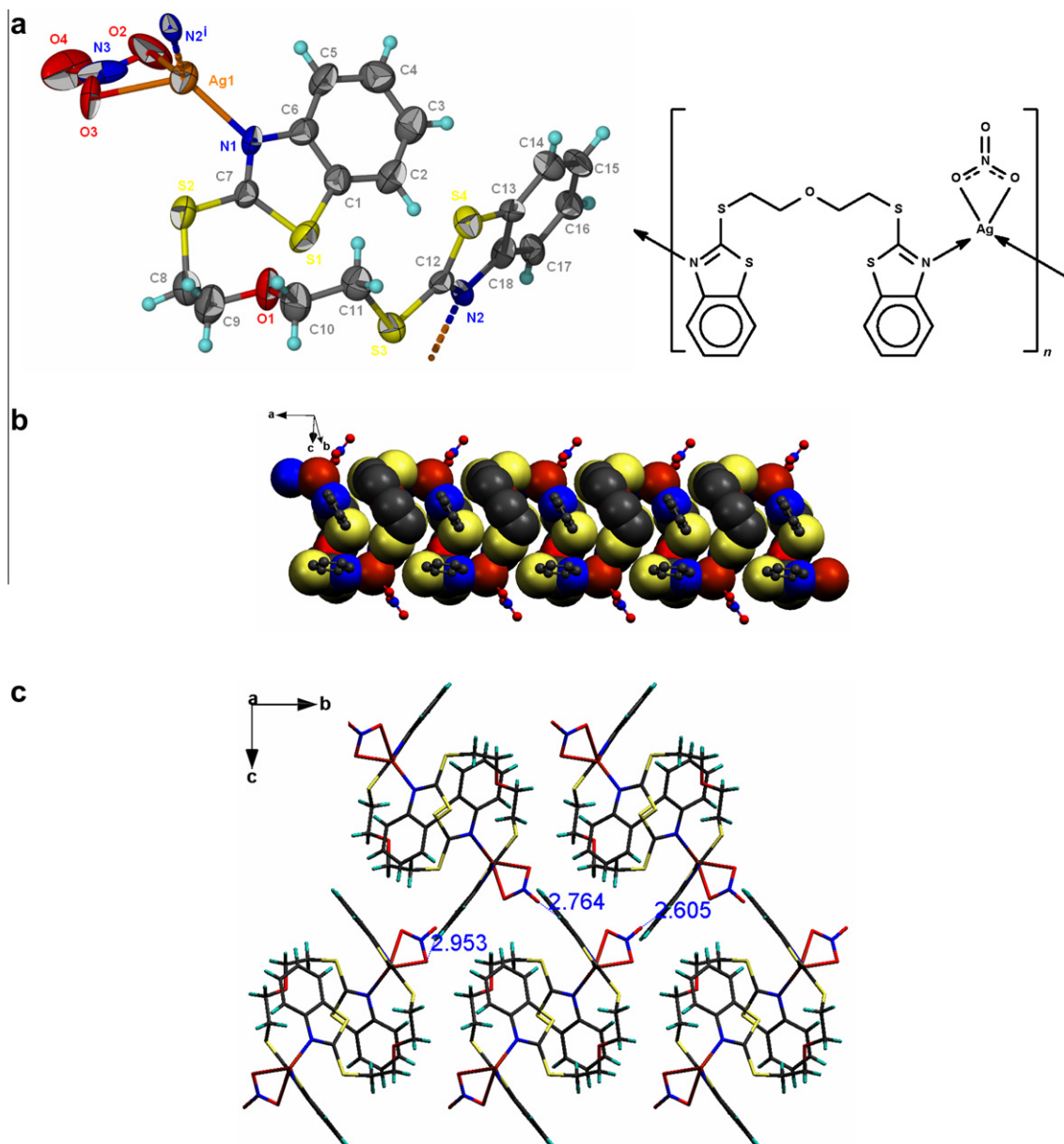


**Fig. 3.** (a) Coordination environment of Ag<sup>+</sup> ions in **3**. (b) 1D helix chain of **3**. (c) 3D supramolecular network in **3** linked via C–H...O hydrogen bonds. Partial H atoms omitted for clarity.

features three different frameworks viewing from three different directions (Fig. 4c).

### 3.2. Antimicrobial activities

The percentage inhibition of the cell growth at each sample concentration was calculated according to the Eq. (1):

$$T = \frac{N_0 - N_i}{N_0} \times 100\% \quad (1)$$

where  $T$  = the percentage, inhibition  $N_0$  = number of cells/ml under the control growth;  $N_i$  = number of cells/ml under the growth at each complex concentration.

The prohibit of  $T$  value was plotted against logarithmic value of the complex concentration and the data were analyzed by linear regression (Fig. 5). The  $EC_{50}$ , which represents the concentration of compounds that inhibited visible growth in *P. tricorutum* by

50% was estimated from the regression equation by matching the logarithmic value of concentration that was equivalent to a 50% inhibition ( $T = 50\%$ ). Regression equations and  $EC_{50}$  values are shown in Table 2.

Fig. 5 clearly show that complexes **1–4** have the obvious restraining effects on the growth of *P. tricorutum*. With the increase of concentration of the complex in the nutrient solution,  $T$  value increased. **4** shows the highest antimicrobial activity ( $EC_{50} = 91.7 \mu\text{g/L}$ ) in four complexes, suggesting that longer chain length and benzothiazole N of the ligand could increase the biological activities of the complex.

### 4. Conclusions

By comparing the structures of four complexes, it is clear that the pyridine (benzothiazole) rings are brought to rotate with the pyridine (benzothiazole) N, and the adjacent S atom adopts a

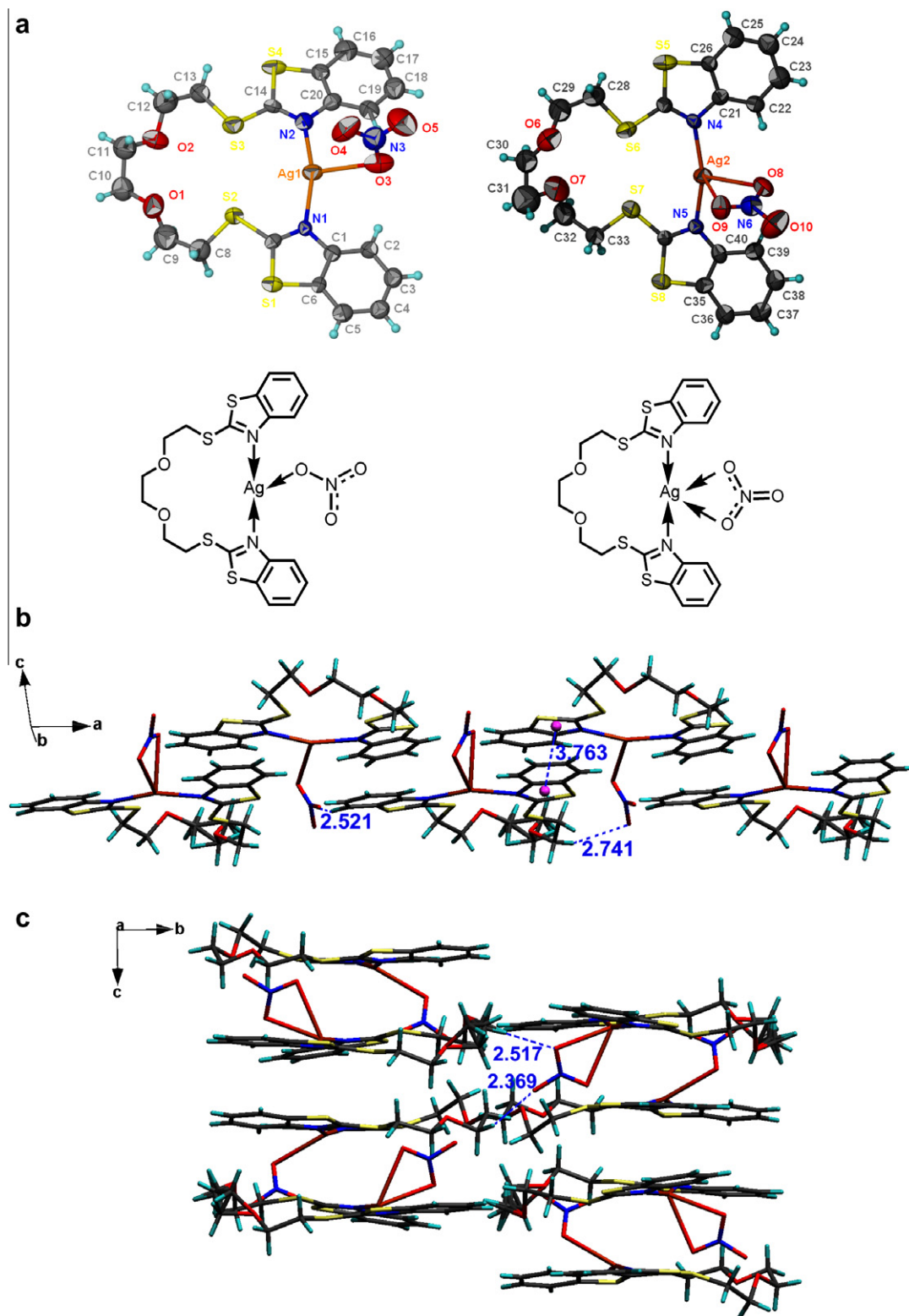


**Fig. 4.** (a) Coordination environment of Ag<sup>I</sup> ions in **4**. (b) 1D chain of **4** via C–H...O hydrogen bonds and  $\pi$ – $\pi$  interactions. (c) 3D supramolecular network in **4** linked via C–H...O hydrogen bonds,  $\pi$ – $\pi$  interactions and weak Ag...S interactions.

*cis*-form when the ligands coordinate to Ag<sup>I</sup> ions, owing to that geometrical effects seem to be more important than electronic effects in these systems. In addition to the strong coordination bonds, there exist other interactions including weak hydrogen bonds, weak Ag...S interactions and  $\pi$ – $\pi$  stacking interactions. These weak interactions play a crucial role in the self-assembly

of supramolecular structures as well as the stabilization of the complex structures in the solid state.

From the differences between **1** and **2**, **3** and **4**, we can see that changes of the (CH<sub>2</sub>CH<sub>2</sub>O)<sub>n</sub> ligands spacers cause subtle geometrical differences in the structure of these complexes, and the effect of ligands spacers is more obvious for ligands **L**<sup>3</sup> and **L**<sup>4</sup>, maybe due to

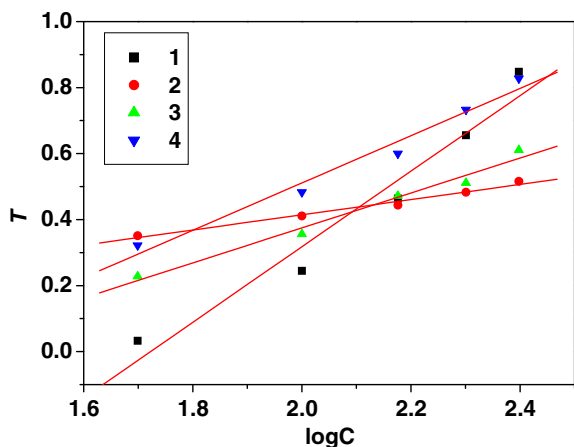


Fig. 5. Semilogarithmic plotting of inhibition effect versus complex concentration in 96-h experiments. Fitted straight lines have also been plotted.

Table 2

Linear equations, correlation coefficient and  $EC_{50}$  values of complexes.

Complex	Linear equation	$R^2$	$EC_{50}$ % ( $\mu\text{g/L}$ )
1	$y = 1.144x - 1.971$	0.957	144.5
2	$y = 0.229x - 0.045$	0.983	239.8
3	$y = 0.529x - 0.685$	0.981	173.8
4	$y = 0.715x - 0.921$	0.974	97.1

the bigger stereo-hindrance effect of the terminal benzothiazole group. Meanwhile, comparing the structures of **1** with **3**, **2** with **4**, indicate that the terminal groups seem to affect the frameworks of these complexes. In general, the effects of terminal groups are more important than ligands spacers.

From the Antimicrobial activity tests we can see that four complexes show different inhibitory effects to the growth of *P. tricornutum* following the order of **4** > **1** > **3** > **2** though it is risky to correlate the bioactivity of these compounds to the structural features. The work to prepare more polynuclear compounds and correlate the relationship between the supramolecular structure and antibacterial activity is in progress in our laboratory.

## Acknowledgments

The authors thank Shanghai Natural Science Foundation (11ZR1414800), "Chen Guang" project supported by Shanghai Municipal Education Commission and Shanghai Education Development Foundation (09CG52), the Project of Shanghai Municipal

Education Commission (09YZ245, 10YZ111), Shanghai Maritime University (20110017, 20110013) for financial support.

## Appendix A. Supplementary material

Supplementary data associated with this article can be found, in the online version, at doi:10.1016/j.ica.2011.06.026. CCDC 809460, 809461, 809462 and 809463 contain the supplementary crystallographic data for this paper. These data can be obtained free of charge from The Cambridge Crystallographic Data Centre via [www.ccdc.cam.ac.uk/data\\_request/cif](http://www.ccdc.cam.ac.uk/data_request/cif).

## References

- [1] D.A. McMoran, P.J. Steel, Chem. Commun. (2002) 2120.
- [2] Z. Huang, M. Du, H.B. Song, X.H. Bu, Cryst. Growth Des. 4 (2004) 71.
- [3] M.C. Hong, Y.J. Zhao, W.P. Su, R. Cao, M. Fujita, Z.Y. Zhou, A.S.C. Chan, Angew. Chem., Int. Ed. 39 (2000) 2468.
- [4] A.J. Blake, N.R. Champness, P.A. Cooke, J.E.B. Nicolson, Chem. Commun. (2000) 665.
- [5] A.S. Kazachenko, A.V. Legler, O.V. Per'yanova, Yu.A. Vstavskaya, Pharm. Chem. J. 34 (2000) 257.
- [6] A. Kascatan-Nebioglu, A. Melaiye, K. Hindi, S. Durmus, M.J. Panzner, L.A. Hogue, R.J. Mallett, C.E. Hovis, M. Coughenour, S.D. Crosby, A. Milsted, D.L. Ely, C.A. Tessier, C.L. Cannon, W.J. Youngs, J. Med. Chem. 49 (2006) 6811.
- [7] Doug A. Medvetz, Khadijah M. Hindi, Matthew J. Panzner, Andrew J. Ditto, Yang H. Yun, Wiley J. Youngs, Met. Based Drugs. 384010 (2008) 7.
- [8] I. Özdemir, E.Ö. Özcan, S. Günel, N. Gürbüz, Molecules 15 (2010) 2499.
- [9] A. Cuin, A.C. Massabni, C.Q.F. Leite, D.N. Sato, A. Neves, B. Szpoganicz, M.S. Silva, A.J. Bortoluzzi, J. Inorg. Biochem. 101 (2007) 291.
- [10] Q. Yu, Y.F. Zeng, J.P. Zhao, Q. Yang, X.H. Bu, Cryst. Growth Des. 10 (2010) 1878.
- [11] J.R. Black, N.R. Champness, W. Levason, G. Reid, J. Chem. Soc., Chem. Commun. (1995) 1277.
- [12] B. Schmaltz, A. Jouaiti, M.W. Hosseini, A. De Cian, Chem. Commun. (2001) 1242.
- [13] P. Grosshans, A. Jouaiti, V. Bulach, J.-M. Planeix, M.W. Hosseini, N. Kyritsakas, Eur. J. Inorg. Chem. (2004) 453.
- [14] A.Y. Robin, J.L. Sagué Doimeadios, A. Néels, T. Vig Slenters, K.M. Fromm, Inorg. Chim. Acta 360 (2007) 212.
- [15] R.D. Bergougnant, A.Y. Robin, K.M. Fromm, Cryst. Growth Des. 5 (2005) 1691.
- [16] J.R. Black, N.R. Champness, W. Levason, G. Reid, Inorg. Chem. 35 (1996) 4432.
- [17] A.J. Blake, N.R. Champness, S.M. Howdle, P.B. Webb, Inorg. Chem. 39 (2000) 1035.
- [18] F.K. Gormley, J. Gronbach, S.M. Draper, A.P. Davis, J. Chem. Soc., Dalton Trans. (2000) 173.
- [19] J.R. Black, W.S. Li, Schröder, M. Lipopolis, Chem. Commun. (1997) 1943.
- [20] X.H. Bu, W.F. Hou, M. Du, W. Chen, R.H. Zhang, Cryst. Growth Des. 2 (2002) 303.
- [21] M.M. Osman, J. Chem. Tech. Biotechnol. 62 (1995) 46.
- [22] I. Omae, Chem. Rev. 103 (2003) 3431.
- [23] G.M. Sheldrick, SHELXL-97, Program for the Solution of Crystal Structures, University of Göttingen, Göttingen, Germany, 1997..
- [24] G.M., Sheldrick, SHELXL-97, Program for the Refinement of Crystal Structures, University of Göttingen, Göttingen, Germany, 1997..
- [25] A. Bondi, J. Phys. Chem. 68 (1964) 441.
- [26] G.A. Jeffrey, Crystallogr. Rev. 9 (2003) 135.
- [27] Y.B. Xie, X.H. Bu, J. Cluster Sci. 14 (2003) 471.
- [28] L. Carlucci, G. Ciani, D.M. Proserpio, A. Sironi, Inorg. Chem. 37 (1998) 5941.
- [29] X.H. Bu, Y.B. Xie, J.R. Li, R.H. Zhang, Inorg. Chem. 42 (2003) 7422.
- [30] D.L. Reger, R.F. Semeniuc, V. Rassolov, M.D. Smith, Inorg. Chem. 43 (2004) 537.